Earth and Planetary Science Letters 391 (2014) 201–211

Contents lists available at ScienceDirect

Earth and Planetary Science Letters

www.elsevier.com/locate/epsl

Evidence for Mo isotope fractionation in the solar nebula and during planetary differentiation

Christoph Burkhardt [a,*], Remco C. Hin [a,1], Thorsten Kleine [b], Bernard Bourdon [c]

[a] Institute of Geochemistry and Petrology, Clausiusstrasse 25, ETH Zürich, CH-8092 Zürich, Switzerland
[b] Institut für Planetologie, Westfälische Wilhelms-Universität Münster, Wilhelm Klemm-Strasse 10, 48149 Münster, Germany
[c] Laboratoire de Géologie de Lyon, ENS Lyon and Université Claude Bernard Lyon 1, 46 Allée d'Italie, F-69364 Lyon, France

ARTICLE INFO

Article history:
Received 5 July 2013
Received in revised form 22 January 2014
Accepted 25 January 2014
Available online xxxx
Editor: B. Marty

Keywords:
Mo isotopes
meteorites
solar nebula
core formation
Moon
Mars

ABSTRACT

Mass-dependent Mo isotope fractionation has been investigated for a wide range of meteorites including chondrites (enstatite, ordinary and carbonaceous chondrites), iron meteorites, and achondrites (eucrites, angrites and martian meteorites), as well as for lunar and terrestrial samples. Magmatic iron meteorites together with enstatite, ordinary and most carbonaceous chondrites define a common $\delta^{98/95}$Mo value of -0.16 ± 0.02‰ (relative to the NIST SRM 3134 Mo standard), which is interpreted to reflect the Mo isotope composition of bulk planetary bodies in the inner solar system. Heavy Mo isotope compositions for IAB iron meteorites most likely reflect impact-induced evaporative losses of Mo from these meteorites. Carbonaceous chondrites define an inverse correlation between $\delta^{98/95}$Mo and metal content, and a positive correlation between $\delta^{98/95}$Mo and matrix abundance. These correlations are mainly defined by CM and CK chondrites, and may reflect the heterogeneous distribution of an isotopically light metal and/or an isotopically heavy matrix component in the formation region of carbonaceous chondrites. Alternatively, the elevated $\delta^{98/95}$Mo of the CM and CK chondrites could result from the loss of volatile, isotopically light Mo oxides, that formed under oxidized conditions typical for the formation of these chondrites.

The Mo isotope compositions of samples derived from the silicate portion of differentiated planetary bodies are heavy compared to the mean composition of chondrites and iron meteorites. This difference is qualitatively consistent with experimental evidence for Mo isotope fractionation between metal and silicate. The common $\delta^{98/95}$Mo values of -0.05 ± 0.03‰ of lunar samples derived from different geochemical reservoirs indicate the absence of significant Mo isotope fractionation by silicate differentiation or impact metamorphism/volatilization on the Moon. The most straightforward interpretation of the Mo isotope composition of the lunar mantle corresponds to the formation of a lunar core at a metal–silicate equilibration temperature of 1800 ± 200 °C. The investigated martian meteorites, angrites and eucrites exhibit more variable Mo isotope compositions, which for several samples extend to values above the maximum $\delta^{98/95}$Mo $= +0.14$‰ that can be associated with core formation. For these samples post-core formation processes such as partial melting, metamorphism and in the case of meteorite finds terrestrial weathering must have resulted in Mo isotope fractionation. Estimates of the metal–silicate equilibration temperatures for Mars (2490 ± 770 °C) and the angrite parent body (1790 ± 230 °C) are thus more uncertain than that derived for the Moon. Although the Mo isotope composition of the bulk silicate Earth has not been determined as part of this study, a value of $-0.16‰ < \delta^{98/95}\text{Mo} < 0$ can be predicted based on the chondrite and iron meteorite data and by assuming a reasonable temperature range for core formation in the Earth. This estimate is in agreement with four analyzed basalt standards (-0.10 ± 0.10). Improved application of mass-dependent Mo isotope fractionation to investigate core formation most of all requires an improved understanding of potential Mo isotope fractionation during processes not related to metal–silicate differentiation.

1. Introduction

Mass-dependent isotope variations among meteorites and their components have been reported for a variety of elements, including S (Gao and Thiemens, 1993), Zn, Cu, and Ni (Luck et al., 2005; Moynier et al., 2006), Cd (Wombacher et al., 2008), Cr

* Corresponding author. Present address: Origins Laboratory, Department of Geophysical Sciences, The University of Chicago, IL 60637, USA. Tel.: +1 773 798 7251; fax: +1 773 702 9505.
E-mail address: burkhardt@uchicago.edu (C. Burkhardt).
[1] Present address: School of Earth Sciences, University of Bristol, Wills Memorial Building, Queen's Road, Bristol BS8 1RJ, UK.

0012-821X/$ – see front matter
http://dx.doi.org/10.1016/j.epsl.2014.01.037

(Moynier et al., 2011), Si (Armytage et al., 2011; Fitoussi et al., 2009; Savage and Moynier, 2013), Ca (Simon and DePaolo, 2010), and Sr (Charlier et al., 2012; Moynier et al., 2010; Patchett, 1980). These isotopic variations have been interpreted to reflect fractionation by condensation/evaporation in the nebula and subsequent uneven mixing of the fractionated nebular reservoirs and their products, particularly Ca,Al-rich inclusions (Luck et al., 2005; Moynier et al., 2010; Simon and DePaolo, 2010) or Si-bearing metal (Savage and Moynier, 2013). More recently, mass-dependent isotope fractionation has also been applied to investigate the conditions of planetary core formation. For instance, the Si and Cr isotope compositions of the bulk silicate Earth are fractionated compared to primitive meteorites, and this has been interpreted to indicate Si and Cr partitioning into the Earth's core (Armytage et al., 2011; Fitoussi et al., 2009; Georg et al., 2007; Hin et al., 2014; Moynier et al., 2011; Shahar et al., 2011). Since the magnitude of isotope fractionation depends on the temperature of metal–silicate equilibration, such isotope studies can potentially provide new constraints on the conditions of core formation.

Molybdenum is an interesting element to add to the studies of mass-dependent isotope fractionation in meteoritic and planetary materials. It is refractory and moderately siderophile, and is composed of seven stable isotopes. Mass-independent (i.e., nucleosynthetic) Mo isotope variations in meteorites and their components are well documented and have been used to investigate mixing processes in the solar nebula as well as genetic relationships among meteorites and between meteorites and the larger terrestrial planets (Burkhardt et al., 2011, 2012; Dauphas et al., 2002, 2004). The elemental distribution of Mo in meteorites is dominated by its affinity for the metal phase, but also by its highly refractory character leading to strong enrichments in Ca,Al-rich inclusions (CAI). Although Mo is refractory under the canonical conditions of the solar nebula, it is less enriched than other highly refractory metals in some CAI from the Allende meteorite. This has been interpreted to reflect removal of volatile Mo oxides formed in oxidizing environments (Fegley and Palme, 1985). During planetary differentiation, Mo preferentially partitions into the core and is strongly depleted in the silicate mantle (e.g., Holzheid and Palme, 2007; Newsom and Palme, 1984; Newsom, 1985, 1986; Righter et al., 1998; Wade et al., 2012; Walter and Thibault, 1995). The magnitude of Mo depletion in the mantle, therefore, can help to assess the pressure, temperature and oxygen fugacity conditions of metal segregation during planetary differentiation (e.g., Wood et al., 2006; Wade et al., 2012).

So far little is known about mass-dependent Mo isotope fractionation during high-temperature processes. This contrasts with the large body of work on such fractionation during low-temperature processes (e.g., Anbar, 2004). In a companion study we have performed liquid-metal liquid-silicate experiments, which demonstrate significant Mo isotope fractionation between metal and silicate up to temperatures of ~3000 °C (Hin et al., 2013). The temperature dependence of this fractionation makes Mo isotopes a tracer to investigate the temperature conditions during planetary core formation.

Here, we present Mo stable isotope data for a variety of chondrites, achondrites, iron meteorites, and lunar samples. These data are used to evaluate the nature and extent of mass-dependent Mo isotope fractionation by solar nebula processes and during planetary differentiation, and to assess whether Mo isotopes can serve as a new tracer for core formation in the terrestrial planets.

2. Analytical methods

2.1. Sample preparation and Mo separation

The samples investigated for this study include eleven chondrites (CV, CM, CO, CR, CK, CB, ordinary and enstatite chondrites), seven iron meteorites (IAB, IIAB, IIIAB, IVA, IVB), three angrites, four eucrites, two martian meteorites, and five lunar samples. In addition four terrestrial basaltic rock standards were analyzed (BHVO-2, BIR-1, W-2a, DNC-1). Whereas the terrestrial rock standards were obtained as powders, all other samples were received as small pieces. They were carefully cleaned with abrasive paper and by sonication in distilled water and ethanol. Several of the meteorite samples are desert finds (Dhofar007, DaG476, NWA4801, NWA4590) and show signs of terrestrial alteration, such as oxidation veins along cracks. When possible, obviously altered parts of these samples were avoided. For NWA4801 this was not possible, however, and for this sample only the grain-size larger than 40 µm was used. All silicate-rich samples were powdered in an agate mortar or mill. For the chondrites Daniel's Kuil, Kernouvé, Allende, Murchison-a and NWA801 aliquots from powders analyzed previously for mass-independent (i.e., nucleosynthetic) Mo isotope anomalies (Burkhardt et al., 2011) were used. The KREEP-rich sample 68115 is the remainder from a W isotope study (Touboul et al., 2007), for which some metal was separated from the powder.

All samples were weighed into 60 ml Savillex beakers, spiked with a ^{100}Mo–^{97}Mo tracer (Hin et al., 2013), and digested in HCl (iron meteorites) or HF–HNO_3–$HClO_4$ (6:3:1) (silicate samples) at 180 °C on a hotplate for several days. This procedure ensured complete spike-sample equilibration. Sample sizes were ~50–100 mg for iron meteorites, ~200 mg for chondrites and ~0.5–2 g for silicate samples. After digestion, samples were dried and re-dissolved in HNO_3–H_2O_2 to attack any remaining organics. Molybdenum was separated from the sample matrix using a three-stage ion exchange procedure employing both anion and cation exchange resins (Burkhardt et al., 2011). Molybdenum was first separated from major elements using a cation exchange column (Bio-Rad AG50W-X8) and 1 M HCl–0.1 M HF (see Patchett and Tatsumoto, 1980). Subsequently, any remaining Fe, Ni and a large part of the Ru was separated from Mo on an anion exchange resin (Bio-Rad AG1-X8) with 1 M HF, while Ti, Zr, Hf and W were eluted using different HCl–HF mixtures (Kleine et al., 2004). Finally, Mo together with some remaining Ru is eluted using 3 M HNO_3. The remaining Ru is removed from the Mo fraction using TRU-Spec resin conditioned in 7 M HNO_3, followed by elution of Mo with 0.1 M HNO_3. This last step was repeated using 1 M HCl and 0.1 M HCl instead of 7 M HNO_3 and 0.1 M HNO_3, resulting in Ru/Mo and Zr/Mo $< 3 \times 10^{-5}$ for most samples. Interference corrections were thus generally <0.02‰, and always <0.05‰ (Cape of Good Hope). Total chemistry yields were 60–85%, highlighting the need for double-spiking to obtain accurate mass-dependent Mo isotope data. Total procedural blanks ranged from 0.3 to 0.9 ng Mo, and were negligible for most samples. However, for some Mo-poor silicate samples blank corrections were necessary (see Table 2).

2.2. Mass spectrometry and data reduction

Molybdenum isotope measurements were performed using a *NuInstruments Plasma1700* MC-ICP-MS at ETH Zürich and a ThermoScientific *NeptunePlus* MC-ICP-MS at the University of Münster. On both instruments all seven Mo isotopes were measured simultaneously in static mode, as well as ^{90}Zr (Zürich) or ^{91}Zr (Münster) and ^{99}Ru to monitor potential isobaric interferences. On the *Nu1700*, samples were introduced via a DSN-100 desolvator equipped with a PFA nebulizer having an uptake rate of ~140 µl/min. When normalized to a 100 µl/min uptake rate,

Table 1
Molybdenum concentrations and isotope compositions of chondrites and iron meteorites.

Sample		N[a]	Mo (μg/g)[b]	$\delta^{98/95}Mo_{measured}$[c]	$\varepsilon^{96}Mo_{(7/5)}$[d]	$\delta^{98/95}Mo_{corr}$[e]
Chondrites						
Karoonda	CK4	5	1.43	0.04 ± 0.03	-1.11 ± 0.19	0.12 ± 0.04
Murchison-a[f]	CM2	5	1.19	-0.20 ± 0.03	-2.40 ± 0.09	-0.04 ± 0.06
Murchison-b[f]	CM2	3	1.18	-0.04 ± 0.06	-1.53 ± 0.22	0.06 ± 0.08
Murchison mean	CM2					0.00 ± 0.05
Kainsaz	CO3	3	1.34	-0.18 ± 0.04	-1.05 ± 0.14	-0.11 ± 0.06
NWA2090	CO3	6	1.26	-0.15 ± 0.04	-0.30 ± 0.16	-0.13 ± 0.05
CO mean	CO3					-0.13 ± 0.03
NWA801	CR2	5	1.63	-0.23 ± 0.04	-1.30 ± 0.07	-0.15 ± 0.06
Allende	CV3	4	1.44	-0.26 ± 0.06	-1.24 ± 0.1	-0.18 ± 0.08
Gujba (metal)	CB	6	5.27	-0.26 ± 0.04	-0.69 ± 0.07	-0.21 ± 0.05
Kernauvé	H6	5	1.32	-0.17 ± 0.04	-0.19 ± 0.06	-0.16 ± 0.04
Nulles	H6	5	1.69	-0.17 ± 0.02	-0.19 ± 0.06	-0.15 ± 0.02
Homestead	L5	3	1.06	-0.17 ± 0.06	-0.19 ± 0.06	-0.16 ± 0.06
Daniel's Kuil	EL6	5	1.10	-0.19 ± 0.02	-0.17 ± 0.05	-0.18 ± 0.02
Iron meteorites						
Odessa	IAB	6	6.86	0.22 ± 0.02	0.09 ± 0.12	0.22 ± 0.03
Toluca	IAB	8	6.23	-0.03 ± 0.03	0.09 ± 0.12	-0.03 ± 0.03
Caddo County	IAB	5	6.77	-0.07 ± 0.04	0.09 ± 0.12	-0.08 ± 0.04
Negrillos	IIAB	6	6.43	-0.17 ± 0.02	-0.34 ± 0.05	-0.14 ± 0.03
Henbury	IIIAB	6	5.74	-0.15 ± 0.04	-0.30 ± 0.10	-0.13 ± 0.04
Gibeon	IVA	5	5.47	-0.17 ± 0.04	-0.19 ± 0.08	-0.16 ± 0.04
Cape of Good Hope	IVB	5	22.47	-0.25 ± 0.06	-0.74 ± 0.03	-0.20 ± 0.07
Average (excl. CK, CM, IAB)						-0.16 ± 0.02

[a] Number of isotopic analyses.
[b] Relative uncertainty (2 s.d.) of measurement is <1%.
[c] Measured Mo isotope mass fractionation relative to the NIST SRM3134 Mo standard. Uncertainties correspond to two-sided 95% Student-t distributions ($t_{0.95,n-1}\sigma/\sqrt{n}$).
[d] Nucleosynthetic ε^{96}Mo isotope anomalies from unspiked measurements and internal normalization to $^{97}Mo/^{95}Mo = 0.602083$; data from this study and Burkhardt et al. (2011).
[e] Mo isotope mass fractionation corrected for nucleosynthetic effects using $\delta^{98/95}Mo_{corrected} = \delta^{98/95}Mo_{measured} - \varepsilon^{96}Mo_{(7/5)nucleosynthetic} \times 0.066$. Uncertainties were propagated assuming a 20% uncertainty on the correction.
[f] Data are from two different Murchison sample powders (Murchison-a and Murchison-b).

this setup resulted in a sensitivity of ~180 V/ppm Mo. Sample and standard measurements on the *Nu1700* were usually performed with 70–100 ppb solutions, yielding a total ion beam intensity of $\sim 2 \times 10^{-10}$ A. For measurements with the *Neptune*, a Cetac AridusII desolvator equipped with a PFA nebulizer having an uptake rate of ~80 μl/min was used. When normalized to a 100 μl/min uptake rate, this setup resulted in sensitivities between 250 and 430 V/ppm Mo, so that measurements were made at lower concentrations (20–70 ppb Mo; ~ 1–2.5×10^{-10} A total Mo ion beams) compared to those on the *Nu1700*. The Mo isotope measurements generally consisted of 30 s baseline integrations (made on-peak using the same 0.5 M HNO_3–0.05 M HF solution also used to prepare the sample solutions) and 40 isotope ratio measurements of 5 s each. The sample measurements were bracketed with measurements of the SRM3134 Mo standard to monitor non-exponential drift in the instrument.

For measurements on the *Nu1700*, data reduction and calculation of $\delta^{98/95}$Mo values was performed following the geometrically motivated iteration procedure for the double spike inversion of Siebert et al. (2001). Data reduction of the data obtained on the *Neptune* was made off-line using the "double-spike toolbox" (Rudge et al., 2009), which employs MATLAB's non-linear equation solving routine for the iteration. To ensure that both routines yielded consistent results, some of the *Nu1700* data were reduced using the "double-spike toolbox" and some of the *Neptune* data with the Siebert et al. (2001) iteration. Both methods yield identical results to within 0.005‰.

The Mo isotope data are reported as $\delta^{98/95}Mo_{measured}$ values relative to SRM3134 (see also Section 3.2). These were calculated from the fractionation factor α given by the double spike inversion and corrected for non-exponential fluctuations in the Mo isotope measurements by subtracting the mean $\delta^{98/95}Mo_{measured}$ of bracketing double-spiked SRM3134 standard runs ($\delta^{98/95}Mo_{bSRM}$) using

$$\delta^{98/95}Mo_{measured} \approx -1000\alpha \ln(m_{98}/m_{95}) - \delta^{98/95}Mo_{bSRM}$$

where m_{98} and m_{95} are the atomic weights of ^{98}Mo and ^{95}Mo. Values for $\delta^{98/95}Mo_{bSRM}$ were generally below ±0.05‰. The external reproducibility of the SRM standard measurements over the course of this study is 0.085‰ (2 s.d.) for the *Nu1700* and 0.056‰ (2 s.d.) for the *Neptune*.

3. Results

3.1. Mo concentrations

The Mo concentration and isotope data of chondrites and iron meteorites are reported in Table 1 and the $\delta^{98/95}$Mo values are plotted in Fig. 1. Data for silicate samples are given in Table 2 and $\delta^{98/95}$Mo values are shown in Fig. 2. The Mo concentrations are ~5–22 ppm in iron meteorites, ~1.1–1.7 ppm in chondrites and ~2–240 ppb in extraterrestrial silicate-rich samples, highlighting the siderophile character of Mo. Among the latter, angrites tend to have the highest Mo concentrations of ~100–240 ppb, while the eucrite sample Stannern-a exhibits the lowest concentration with only ~2 ppb Mo. The Mo concentrations obtained in the present study agree to within ~5% with the values reported in Burkhardt et al. (2011) for the same powders/samples. For the angrite NWA 4801 a ~30% lower concentration was determined here compared to our previous work (Burkhardt et al., 2011), and this most likely reflects that the grain size fraction <40 μm was excluded from the analysis in this study. The range of Mo concentrations determined here for eucrites is similar to that obtained in a previous

Table 2
Molybdenum concentrations and isotope compositions of terrestrial basalts, lunar samples and basaltic achondrites.

Sample		N[a]	Mo (ng/g)[b]	$\delta^{98/95}Mo_{measured}$	$\delta^{98/95}Mo_{blank\ corrected}$[c]	$\Delta^{98/95}Mo_{bulk\text{-}silicate}$[d]
Terrestrial basalts						
BHVO-2	Hawaii basalt	23	~4550	−0.06 ± 0.03	−0.06 ± 0.03	−0.10 ± 0.04
W-2a	Virginia diabase	2	393	−0.05 ± 0.06	−0.05 ± 0.06	−0.11 ± 0.06
DNC-1	N-Carolina ol-dolerite	2	121	−0.18 ± 0.06	−0.18 ± 0.06	0.02 ± 0.06
BIR-1	Iceland ol-tholeite	4	32	−0.11 ± 0.03	−0.11 ± 0.03	−0.05 ± 0.04
Basalt mean				−0.10 ± 0.10	−0.10 ± 0.10	−0.06 ± 0.10
Moon						
12004.142	Low-Ti Marebasalt	2	41	−0.09 ± 0.03	−0.06 ± 0.04	−0.10 ± 0.04
15499.159	Low-Ti Marebasalt	1	25	−0.01 ± 0.10	−0.06 ± 0.12	−0.10 ± 0.13
15556.203	Low-Ti Marebasalt	1	16	0.04 ± 0.13	−0.04 ± 0.17	−0.12 ± 0.17
74275.32	High-Ti Marebasalt	1	50	0.01 ± 0.10	−0.01 ± 0.11	−0.15 ± 0.12
68115.112	KREEP-rich breccia	2	83	−0.10 ± 0.03	−0.08 ± 0.03	−0.08 ± 0.04
Moon mean				−0.03 ± 0.07	−0.05 ± 0.03	−0.11 ± 0.04
Mars						
DAG476	Shergottite	2	53	0.43 ± 0.06	0.44 ± 0.06	−0.60 ± 0.07
Zagami	Shergottite	3	50	−0.09 ± 0.07	−0.10 ± 0.07	−0.06 ± 0.07
Angrites						
NWA4801	Angrite	2	100	0.49 ± 0.02	0.50 ± 0.02	−0.66 ± 0.03
D'Orbigny	Angrite	6	136	−0.05 ± 0.04	−0.05 ± 0.04	−0.11 ± 0.05
NWA4590	Angrite	3	243	−0.14 ± 0.04	−0.14 ± 0.04	−0.02 ± 0.04
Eucrites						
Millbillillie	Monomict eucrite	6	7	0.16 ± 0.08	0.24 ± 0.12	−0.40 ± 0.12
Stannern-a	Monomict eucrite	2	2	−0.49 ± 0.37	−0.22 ± 0.51	0.06 ± 0.51
Stannern-b	Monomict eucrite	2	11	−0.34 ± 0.05	−0.39 ± 0.07	0.23 ± 0.07
Stannern mean					−0.30 ± 0.34	0.14 ± 0.34
Béreba	Monomict eucrite	1	3	0.90 ± 0.24	0.92 ± 0.25	−1.08 ± 0.25
Dhofar 007	Cumulate eucrite	4	83	0.26 ± 0.04	0.27 ± 0.04	−0.43 ± 0.05

[a] Number of isotopic analyses.
[b] Relative uncertainty (2 s.d.) of measurement is <1%.
[c] Blank corrected Mo isotope mass fractionation relative to the NIST SRM3134 Mo standard. Blank compositions ranged from −0.7 ± 0.3 (2 s.e.) to 1.0 ± 0.4‰. Uncertainties correspond to two-sided 95% Student-t distributions ($t_{0.95,n-1}\sigma/\sqrt{n}$) for ($n \geqslant 3$) or 2 SE (for $n < 3$) and include a propagated uncertainty of 50% assumed for the blank correction.
[d] $\Delta^{98/95}Mo_{bulk\text{-}silicate} = \delta^{98/95}Mo_{bulk} - \delta^{98/95}Mo_{silicate}$.

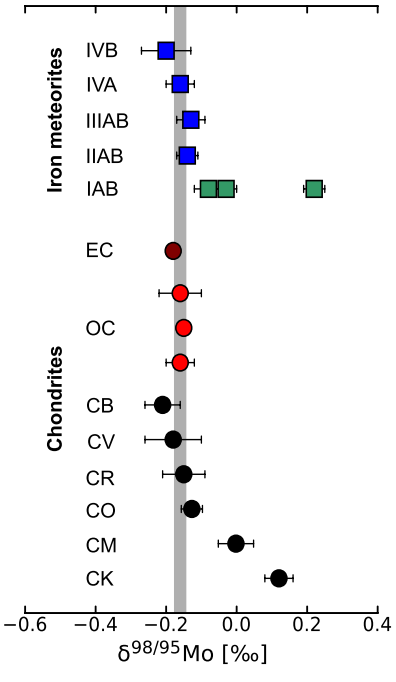

Fig. 1. Mo stable isotope composition of chondrites and iron meteorites. $\delta^{98/95}$Mo calculated relative to the SRM3134 Mo standard and corrected for nucleosynthetic anomalies. Magmatic iron meteorites, enstatite chondrites and ordinary chondrites exhibit a common $\delta^{98/95}$Mo averaging at −0.16 ± 0.02‰. Carbonaceous chondrites have more variable $\delta^{98/95}$Mo, but only the Mo isotope composition of the CM and CK chondrites is significantly heavier compared to that of the magmatic irons, enstatite and ordinary chondrites.

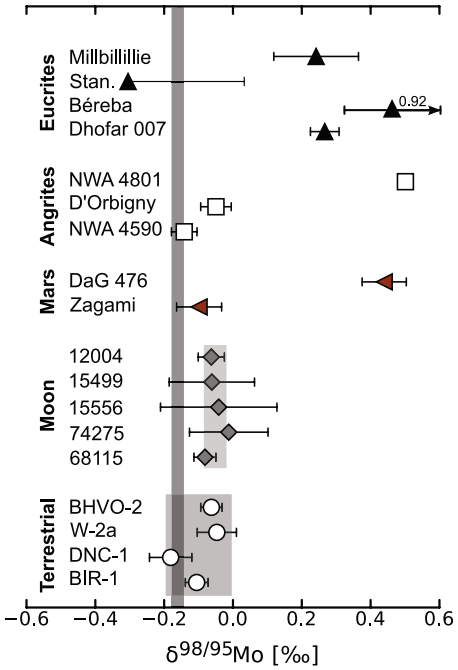

Fig. 2. Mo stable isotope composition of samples derived from the silicate portion of differentiated planetary bodies. $\delta^{98/95}$Mo calculated relative to the SRM3134 Mo standard. Most samples exhibit a heavier Mo isotope composition compared to the chondrite–iron meteorite average, which defines the bulk composition of their parent bodies (gray bar at $\delta^{98/95}Mo = -0.16 \pm 0.02$‰). Stan. = Stannern. Béreba plots at $\delta^{98/95}Mo = 0.92$.

study of eucrites (Newsom, 1985). However, for a given sample the values often vary considerably between and within the studies, indicating heterogeneities (nugget effect) on the sampling scale for these rocks. The lunar samples have Mo concentrations at the lower end of previously reported values (Newsom, 1986). For low-Ti mare basalt 12004 the Mo concentration is about three times lower than that determined by Neal (2001) using another fragment of this rock, and this also is presumably due to sample heterogeneity. Note that the Mo concentration of 44 ppb obtained for the KREEP-rich highland breccia 68115 is only a lower limit because a metal fraction was removed from this sample in a previous study (Touboul et al., 2007).

We have also analyzed four international rock standards and for three of them (BIR-1, DNC-1, W-2a) report the first high-precision Mo concentration data. The BHVO-2 basalt standard was digested five times and each of these digestions was analyzed multiple times. The measured Mo concentrations range from 3.84 to 5.46 ppm, indicating substantial sample heterogeneity even in the BHVO-2 powder. The average concentration of 4.55 ppm obtained from the five independent digestions agrees with literature values (~4 ppm) as reported in the GeoReM database.

3.2. Mo isotope data and $\delta^{98/95}$Mo values

The Mo isotope data are given as $\delta^{98/95}$Mo values calculated relative to the NIST SRM3134 Mo standard, where $\delta^{98/95}Mo_{measured}$ represents the measured isotope fractionation as defined above, while $\delta^{98/95}Mo_{corrected}$ is the purely mass-dependent isotope fractionation obtained after correction for mass-independent (i.e., nucleosynthetic) isotope anomalies. The double spike inversion of a sample run calculates iteratively a fractionation factor α relative to the SRM3134 standard by assuming that the difference in the isotopic composition of the sample and the standard is entirely mass-dependent. However, for samples having nucleosynthetic Mo isotope anomalies, such as iron meteorites and chondrites (Burkhardt et al., 2011; Dauphas et al., 2002), this routine leads to false α values and thus to incorrect $\delta^{98/95}$Mo. Therefore, the contributions of mass-dependent and nucleosynthetic effects to the Mo isotope abundances must be separated. In other words, $\delta^{98/95}Mo_{measured}$ must be corrected for nucleosynthetic effects to obtain the purely mass-dependent Mo isotope fractionation. Although separating mass-dependent and mass-independent contributions can be problematic in some cases (e.g., Niederer et al., 1985), it is straightforward for Mo. This is because both contributions are small (see supplementary material for details), and because it is known which Mo isotopes are affected by mass-independent effects. The latter is known from the comparison of observed Mo isotope anomalies with astrophysical neutron capture models (for details see Burkhardt et al., 2011). To correct for the effects of nucleosynthetic Mo isotope anomalies on measured $\delta^{98/95}$Mo values, the Mo isotope composition of the unspiked samples must be known. For most samples this information was already available from our previous Mo isotope study (Burkhardt et al., 2011), but for the chondrites Karoonda, Murchison-b and Kainsaz Mo isotope measurements on unspiked aliquots were performed in the present study (data and procedures in the supplementary material).

The effects of nucleosynthetic isotope anomalies can be corrected using two different approaches. The first uses the Mo isotope compositions of the samples determined in an unspiked analysis instead of that of the SRM3134 standard in the double spike inversion to obtain "absolute" isotope abundances of the samples (e.g., Niederer et al., 1985). Normalizing those abundances to the ones of the SRM3134 standard and subtracting the mass-independent effect then gives the pure mass-dependent fractionation. In the second approach the $\delta^{98/95}Mo_{measured}$ values obtained from the double spike inversion using the SRM3134 standard composition are subsequently corrected using the independently measured nucleosynthetic isotope anomalies by the following equation:

$$\delta^{98/95}Mo_{corrected} = \delta^{98/95}Mo_{measured} - \varepsilon^{96}Mo_{(7/5)nucleosynthetic} \times 0.066$$

where $\varepsilon^{96}Mo_{(7/5)nucleosynthetic}$ is the nucleosynthetic anomaly for ε^{96}Mo (normalized to ^{97}Mo/^{95}Mo). This equation was derived by modeling the effects of nucleosynthetic *s*-process anomalies (using *s*-process abundances from the stellar model of Arlandini et al., 1999) on the measured $\delta^{98/95}$Mo values. Both correction methods were tested and yield identical results (see supplementary material for a detailed discussion).

Table 1 summarizes the $\delta^{98/95}Mo_{measured}$ values obtained by using the SRM3134 composition in the double spike inversion, and the $\delta^{98/95}Mo_{corrected}$ values corrected for nucleosynthetic Mo isotope anomalies. The largest correction of 0.16‰ was necessary for sample Murchison-a, which was corrected using the nucleosynthetic anomaly measured by Burkhardt et al. (2011) in a separate digestion of the same powder. A different powder of Murchison (Murchison-b), for which spiked and unspiked data were obtained in the present study, gave a slightly heavier $\delta^{98/95}Mo_{measured}$, but also required a smaller correction for nucleosynthetic isotope variations of ~0.10‰. The resulting $\delta^{98/95}Mo_{corrected}$ values of the two Murchison samples agree very well, demonstrating the robustness of the correction procedure. We note, however, that for analyses of primitive chondrites it would be best to obtain unspiked and spiked data from aliquots of a single sample dissolution. After correction, most chondrites and iron meteorites have indistinguishable $\delta^{98/95}$Mo values averaging at -0.16 ± 0.02‰ (95% c.i., $n = 12$), and only the CK and CM chondrites as well as the IAB meteorites exhibit slightly heavier Mo isotope compositions.

No corrections for nucleosynthetic Mo isotope anomalies were necessary for the achondrites and lunar samples, because no resolvable nucleosynthetic Mo isotope anomalies were observed (angrites, martian meteorites) or are expected (eucrites, lunar samples) for these samples (Burkhardt et al., 2011). The lunar samples have indistinguishable Mo isotope compositions and define a mean $\delta^{98/95}$Mo of -0.05 ± 0.03‰, significantly heavier than the mean value for chondrites and iron meteorites. The martian meteorites, angrites and eucrites exhibit more variable $\delta^{98/95}$Mo values ranging from near chondritic (Zagami, NWA 4590, D'Orbigny, Stannern) to very heavy Mo isotope compositions (DaG 476, NWA 4801, Dhofar 007, Béreba, Millbillillie). The terrestrial rock standards exhibit a more restricted range in $\delta^{98/95}$Mo values, which vary between the chondritic composition and slightly heavier values of up to −0.05‰. Note that the $\delta^{98/95}$Mo value of BHVO-2 is well defined (-0.06 ± 0.03‰), indicating that the variable Mo concentrations observed among powder aliquots do not influence measured Mo isotope compositions.

4. Discussion

The new Mo isotope data reveal substantial mass-dependent Mo isotope fractionation among meteorites and lunar and terrestrial samples. Whereas most iron meteorites and chondrites are characterized by uniform $\delta^{98/95}$Mo values (note that in the following we omit subscripts on $\delta^{98/95}$Mo, but always refer to the corrected values) most of the investigated silicate-rich samples exhibit heavier Mo isotope compositions. Qualitatively, this is consistent with evidence from metal–silicate equilibration experiments, which demonstrate that silicates are isotopically heavier than coexisting metal (Hin et al., 2013). Thus, the heavy Mo isotope compositions at least in part seem to result from core formation. However, the variable and sometimes very high $\delta^{98/95}$Mo

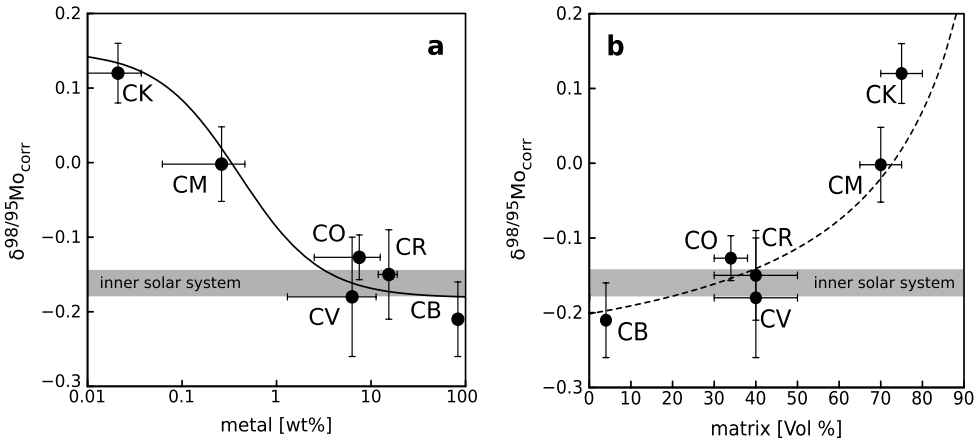

Fig. 3. The stable Mo isotope composition of carbonaceous chondrites is roughly correlated with (a) metal and (b) matrix abundances. Black line in (a) represents mixing of isotopically heavy silicates ($\delta^{98/95}$Mo = 0.15) with light metal ($\delta^{98/95}$Mo = −0.18) and assuming $Mo_{metal}/Mo_{silicate} = 250$; dashed line in (b) represents mixing of isotopically heavy matrix ($\delta^{98/95}$Mo = 0.70) with light non-matrix component ($\delta^{98/95}$Mo = −0.20) and assuming $Mo_{matrix}/Mo_{non\text{-}matrix} = 0.11$. Metal and matrix abundances from Krot et al. (2007).

values observed for some of the achondrites, the IAB irons, and the CM and CK chondrites cannot be interpreted as signatures of core formation, indicating that other processes also resulted in mass-dependent Mo isotope fractionation. Below we discuss potential mechanisms of Mo isotope fractionation in the solar nebula and on meteorite parent bodies, define the $\delta^{98/95}$Mo of bulk planetary bodies in the inner solar system, and explore the magnitude and direction of Mo isotope fractionation during planetary differentiation.

4.1. Molybdenum stable isotope behavior in the solar nebula

All but two of the investigated chondrites have indistinguishable $\delta^{98/95}$Mo values, regardless of their class (EC, OC, CC) and petrologic type (2–6). This implies that processes on the chondrite parent bodies, such as aqueous alteration and thermal metamorphism did not result in significant Mo isotope fractionation. However, the CM and CK chondrites exhibit much higher $\delta^{98/95}$Mo than all other chondrites investigated in this study, implying that processes within the solar nebula resulted in mass-dependent Mo isotope fractionation.

According to the kinetic theory of gases, condensation results in light isotope enrichments in the condensing phase, while the remaining gas will be progressively enriched in heavy isotopes (Chapman and Cowling, 1970). Thus, condensed Mo metal is expected to be isotopically light. For instance, assuming a gas consisting of Mo and H_2, a Mo isotope fractionation of ~0.3‰ can be estimated between gas and Mo condensate, using $\alpha^{98/95} \approx (\mu_{98}/\mu_{95})^{1/2}$ with μ_{98} and μ_{95} being the reduced masses $(m_{98Mo} \times m_{H_2})/(m_{98Mo} + m_{H_2})$ and $(m_{95Mo} \times m_{H_2})/(m_{95Mo} + m_{H_2})$, respectively. Furthermore, experimental evidence suggests that silicates are heavier than coexisting metals (Hin et al., 2013). Thus, among the phases formed in the solar nebula, Mo metal presumably exhibits the lowest $\delta^{98/95}$Mo. Given that most of the Mo probably condensed as metal, a heterogeneous distribution of this metal could potentially be responsible for the $\delta^{98/95}$Mo variations among chondrites. The chondrites indeed exhibit an inverse correlation between $\delta^{98/95}$Mo and metal content (Fig. 3). The CK and CM chondrites have the lowest metal contents and the highest $\delta^{98/95}$Mo among the chondrites, which is consistent with a deficit in isotopically light Mo metal. However, a heterogeneous distribution of Mo-rich metal would also result in variable Mo contents among the different chondrites, and also in a correlation between $\delta^{98/95}$Mo and Mo content. This is illustrated by calculating a mixing curve between presumed metal and silicate end members,

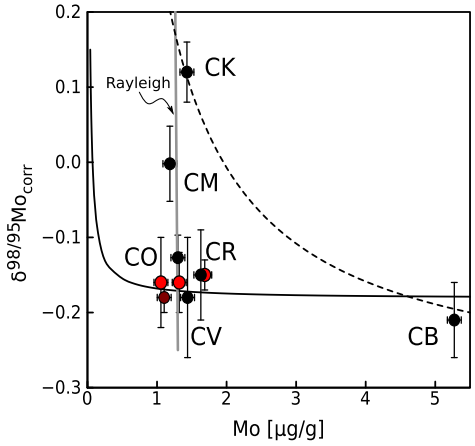

Fig. 4. $\delta^{98/95}$Mo vs. Mo content of chondrites. Symbols as in Fig. 1. Calculated mixing lines between metal and silicate (black line) and matrix and non-matrix components (dashed line) are the same as in Fig. 3. The mixing lines do not reproduce the variable Mo concentration of chondrites, indicating that simple mixing is not the sole cause of the observed Mo isotope variations. In contrast, Rayleigh fractionation (gray line) can account for both, the spread in $\delta^{98/95}$Mo observed among the investigated chondrites and the near constant Mo contents of the bulk chondrites (note that for CB chondrites only the metal was analyzed).

which show that a heterogeneous distribution of Mo-rich metal cannot easily account for the variable $\delta^{98/95}$Mo and near constant Mo contents observed for chondrites (Fig. 4). It is noteworthy that Karoonda (CK4) exhibits the highest $\delta^{98/95}$Mo among chondrites and also has one of the highest Mo contents. This is not easily reconciled with a deficit of isotopically light (and presumably Mo-rich) metal as the sole origin of the heavy Mo isotope composition of the CK (and CM) chondrites. One reason that the Mo concentration, metal abundance and Mo isotopic composition of chondrites cannot be easily fitted by simple two component mixing calculations might be that the Mo content of the metal and silicate matrix phases changes as the meteorites get more oxidized.

Fig. 3 illustrates that $\delta^{98/95}$Mo of the chondrites is not only correlated with metal content, but also with the abundance of matrix. Thus, the Mo isotope variations observed among the chondrites could in principle also reflect mixing with a matrix component characterized by a heavy Mo isotope composition. However, as for the mixing of metal and silicate, such mixing calculations cannot easily account for the near constant Mo contents of the chondrites (Fig. 4). In any case, the origin of the putative matrix-

component remains enigmatic, making this model difficult to test. Clearly, Mo isotope analyses of matrix-rich samples and chondrite metals would be important to assess the role of these components in defining the bulk $\delta^{98/95}$Mo of chondrites.

Although Mo is highly refractory under reduced conditions, it becomes increasingly volatile in more oxidized environments (Fegley and Palme, 1985). Thus, the Mo isotope variations among chondrites could potentially also result from evaporative loss of volatile Mo oxides. The latter are expected to be isotopically light, such that an evaporative loss of Mo would leave behind a heavier residue. It is noteworthy that the CK and CM chondrites formed under more oxidized conditions than the other chondrites investigated for this study, and as such may have lost a larger fraction of volatile Mo oxides. This is, at least in a qualitative sense, consistent with the fact that these two chondrites exhibit the heaviest Mo isotope composition among the investigated chondrites. The isotopic effects of evaporative losses of Mo can be evaluated using the Rayleigh fractionation equation

$$R = R_0 \cdot f^{\alpha-1}$$

where R is the isotopic ratio (here ^{98}Mo/^{95}Mo), R_0 is the initial ratio, f is the fraction of Mo remaining, and $\alpha = (m_{^{95}MoO_2}/m_{^{98}MoO_2})^{1/2}$ is the fractionation factor, assuming that MoO_2 is the main volatile species. Using this equation it can be shown that the $\delta^{98/95}$Mo value is changed by ~0.3‰ while only ~3% of the Mo is lost. Thus, Rayleigh fractionation can account for the spread in $\delta^{98/95}$Mo observed among the investigated chondrites without significantly affecting the Mo content of the bulk chondrites, and as such is consistent with the observed Mo isotope systematics of the chondrites (Fig. 4).

In summary, the variable Mo isotope compositions of carbonaceous chondrites most likely reflect mass-dependent Mo isotope fractionation in the solar nebula, but the processes responsible for this fractionation remain poorly constrained. The two most likely causes are (i) heterogeneous distribution of an isotopically light metal or an isotopically heavy matrix component, and (ii) evaporative losses of isotopically light Mo oxides under oxidized conditions. Clearly, the investigation of mass-dependent Mo isotope fractionation between different chondrite components will be important for identifying the origins of the variable $\delta^{98/95}$Mo in bulk carbonaceous chondrites.

4.2. Bulk $\delta^{98/95}$Mo of the inner solar system

An intriguing observation from the Mo isotope data is that the ordinary, enstatite and most of the carbonaceous chondrites exhibit a common Mo isotope composition that is also indistinguishable from that of magmatic iron meteorites. Owing to its siderophile character, the majority of the Mo resides in the metallic core of planetary bodies, such that the $\delta^{98/95}$Mo of the iron meteorites closely approximate that of the bulk parent body. This can be illustrated by simple mass balance, which requires that

$$\delta^{98/95}\mathrm{Mo_{core}} = \delta^{98/95}\mathrm{Mo_{bulk}} + X_{\mathrm{mantle}}/(1 - X_{\mathrm{mantle}}) \times 1/D_{\mathrm{Mo}}\left(\delta^{98/95}\mathrm{Mo_{bulk}} - \delta^{98/95}\mathrm{Mo_{mantle}}\right)$$

where D_{Mo} is the metal–silicate partition coefficient. Since the Mo isotope fractionation between metal and silicate during core formation is expected to be small (<0.3‰ at temperatures >1000 °C; Hin et al., 2013), and assuming a mass fraction of the mantle of $X_{\mathrm{mantle}} = 0.68$, mass balance indicates that for $D_{\mathrm{Mo}} > 20$ the $\delta^{98/95}$Mo values of the bulk body and that of the core are indistinguishable at the current level of analytical precision (i.e., ±0.02‰ $\delta^{98/95}$Mo) (Fig. 5). Given that D_{Mo} is likely >100 (e.g., Palme and O'Neill, 2003), the $\delta^{98/95}$Mo of the magmatic iron meteorites must reflect those of their parent bodies. The common $\delta^{98/95}$Mo of magmatic irons, enstatite, ordinary, and most carbonaceous chondrites, therefore, indicates that bulk planetary bodies in the inner solar system are characterized by a homogeneous Mo isotope composition, which is given by the mean $\delta^{98/95}\mathrm{Mo_{bulk}}$ of -0.16 ± 0.02‰ (95% c.i.) of these samples.

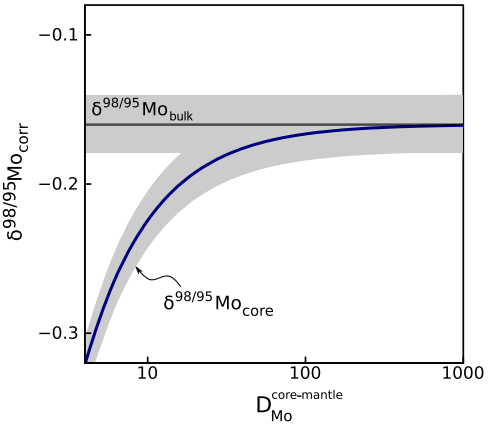

Fig. 5. $\delta^{98/95}$Mo vs. metal–silicate partition coefficient (D_{Mo}). Within the current uncertainty of the Mo isotope measurements of 0.02‰ the Mo isotope composition of the metal core is indistinguishable from that of the bulk body, if D_{Mo}>20.

4.3. IAB iron meteorites and impact-induced Mo isotope fractionation

The IAB iron meteorites exhibit a heavier and more variable Mo isotope composition compared to other iron meteorites. This is consistent with the classification of this group as 'non-magmatic' iron meteorites (Wasson, 1985), indicating that they likely formed by other processes than the magmatic irons and do not represent pristine samples of crystallized asteroidal core material. Several formation models have been proposed for the IAB irons including formation in impact melt pools, disruption and reassembly of a partially differentiated parent body, and crystallization of a S-rich metal melt (Benedix et al., 2000; Choi et al., 1995; Kracher, 1985). Most of these models have in common that impact processes played a dominant role in the genesis of IAB irons. This is consistent with the Mo isotope data, because the heavy and variable Mo isotope compositions of the IAB irons can readily be explained by evaporative losses of isotopically light Mo during energetic impact processes. This is in line with light and variable Ge isotope compositions (Luais, 2007) and a negative correlation between δ^{66}Zn and Zn concentrations (Chen et al., 2013) in IAB irons, which were also interpreted to reflect evaporative losses during impacts. As shown in Section 4.1, Mo losses of less than a few percent are sufficient to account for the observations. In contrast, the segregation of a S-rich core is more difficult to reconcile with the heavy and variable Mo isotope compositions, because all magmatic irons show homogeneous Mo isotope compositions, in spite of their variable S contents. The Mo isotope data, therefore, provide additional support for the hypothesis that the non-magmatic irons formed by fundamentally different processes than magmatic iron meteorites.

4.4. Mo isotope fractionation during planetary core formation

The $\delta^{98/95}$Mo representative of the bulk silicate portion of a differentiated planetary body in conjunction with the experimental determination of the equilibrium fractionation between liquid metal and liquid silicate (Hin et al., 2013) can be used to constrain the temperature of metal–silicate segregation during planetary differentiation. This approach assumes complete metal–silicate

equilibrium and quantitative metal segregation during core formation. The latter is required because if significant amounts of metal had remained in the silicate mantle, then the Mo isotope composition of the mantle would entirely be dominated by the metal. At least for the terrestrial planets, efficient metal segregation almost certainly occurred. This is because accretion of the terrestrial planets is thought to have involved several giant impacts, which released sufficient energy to cause global melting, facilitating efficient metal–silicate segregation in a magma ocean (Rubie et al., 2007; Stevenson, 2008).

The temperature (in Kelvin) of metal–silicate equilibration can be calculated from the Mo isotope data using:

$$T = \sqrt{\left[(-4.70 \pm 0.59) \times 10^5 / \Delta^{98/95}\mathrm{Mo}_{\mathrm{metal-silicate}}\right]}$$

(Hin et al., 2013), where $\Delta^{98/95}\mathrm{Mo}_{\mathrm{metal-silicate}}$ is the difference between the Mo isotope composition of the metal core and the silicate mantle,

$$\Delta^{98/95}\mathrm{Mo}_{\mathrm{metal-silicate}} = \delta^{98/95}\mathrm{Mo}_{\mathrm{core}} - \delta^{98/95}\mathrm{Mo}_{\mathrm{mantle}}$$

which for mass-balance reasons (see above) is approximately the same as:

$$\Delta^{98/95}\mathrm{Mo}_{\mathrm{bulk-silicate}} = \delta^{98/95}\mathrm{Mo}_{\mathrm{bulk}} - \delta^{98/95}\mathrm{Mo}_{\mathrm{mantle}}$$

Based on chondrite and iron meteorite data, the Mo isotope composition of bulk planetary bodies is $\delta^{98/95}\mathrm{Mo}_{\mathrm{bulk}} = -0.16 \pm 0.02‰$, and so determining $\delta^{98/95}\mathrm{Mo}_{\mathrm{mantle}}$, i.e., the Mo isotope composition characteristic for the bulk silicate portion of a planetary body, would allow determining an average temperature of metal–silicate equilibration.

From the above equation it follows that $\Delta^{98/95}\mathrm{Mo}_{\mathrm{bulk-silicate}}$ is ~0.3‰ at $T = 1000\,^{\circ}\mathrm{C}$ (i.e., the minimum temperature for core formation, for which at least the metal must be molten) and decreases with increasing temperature of metal–silicate equilibration. Thus, the largest equilibrium Mo isotope fractionation that can be associated with core formation is ~0.3‰ (assuming single stage core formation and a chondritic parent body). Consequently, if $\delta^{98/95}\mathrm{Mo}_{\mathrm{bulk}} = -0.16‰$, then the $\delta^{98/95}\mathrm{Mo}_{\mathrm{mantle}}$ value characteristic for the bulk silicate portion of a differentiated body can at most be +0.14‰. However, several of the differentiated achondrites analyzed for this study (eucrites, angrite NWA 4801, shergottite DaG 476) exhibit more elevated $\delta^{98/95}\mathrm{Mo}$ values than this maximum $\delta^{98/95}\mathrm{Mo}$ permitted for a core formation signature, indicating that their Mo isotope composition does not only reflect core formation, but has been modified by other processes.

4.4.1. Moon

The five lunar samples analyzed for the present study have indistinguishable Mo isotope compositions averaging at $\delta^{98/95}\mathrm{Mo} = -0.05 \pm 0.03‰$ (95% c.i., $n = 5$). The samples derive from different lunar geochemical reservoirs (low-Ti and high-Ti mare basalts, KREEP) and formed by different magmatic processes on the Moon. Their homogeneous $\delta^{98/95}\mathrm{Mo}$ indicates that Mo isotope fractionation during igneous processes on the Moon was minor to absent. The $\delta^{98/95}\mathrm{Mo}$ of the lunar samples can thus be assumed to represent that of the bulk silicate Moon.

The interpretation of the bulk lunar $\delta^{98/95}\mathrm{Mo}$ in terms of core formation is complicated, however, because the Moon has non-chondritic abundances of refractory siderophile elements (such as Mo) and may have lost some elements by volatilization during impact. According to the giant impact hypothesis, the Moon predominantly consists of silicate mantle material derived from the impactor (Canup, 2004) and/or the proto-Earth (Canup, 2012; Cuk and Stewart, 2012; Reufer et al., 2012). The precursor material of the Moon, therefore, had already undergone core formation and as such might have had an already fractionated Mo isotope composition. However, there is strong evidence that the Moon has a metallic core (Weber et al., 2011) and numerical simulations of the Moon-forming impact suggest that some impactor core material was remixed with the mantle material and was ultimately included into the Moon (Canup, 2004). This core material almost certainly had chondritic $\delta^{98/95}\mathrm{Mo}$ and, owing to the strongly siderophile character of Mo, was strongly enriched in Mo. The Mo isotope composition of the bulk Moon, therefore, most likely was dominated by this core component and hence had chondritic $\delta^{98/95}\mathrm{Mo}$.

It is more difficult to assess whether the lunar Mo isotope data have been affected by volatilization of Mo during the giant impact (O'Neill, 1991). The evaporation of Mo might have caused a preferential loss of isotopically light Mo from the Moon, but more volatile and lighter elements such as Li (Magna et al., 2006), K (Humayun and Clayton, 1995) and Si (Armytage et al., 2012; Fitoussi and Bourdon, 2012) do not show significant isotopic fractionation between the Earth and Moon. Thus, although isotopic fractionation associated with evaporative losses of Mo from the Moon cannot be excluded, there is currently no supportive isotopic evidence for such a scenario.

The most straightforward interpretation of the lunar Mo isotope data is that the bulk lunar $\delta^{98/95}\mathrm{Mo}$ is a signature of core formation. If this is correct, then the lunar mantle is characterized by $\Delta^{98/95}\mathrm{Mo}_{\mathrm{bulk-silicate}} = -0.11 \pm 0.04‰$, which would translate to a metal–silicate equilibration temperature of $1800 \pm 200\,^{\circ}\mathrm{C}$. This temperature estimate is in good agreement with independent estimates based on the partitioning of siderophile elements (Righter, 2002), demonstrating the potential of Mo isotopes as a new tool to constrain the (temperature) conditions of core formation.

4.4.2. Mars and differentiated asteroids

To investigate potential mass-dependent Mo isotope fractionation during core formation in Mars and the parent bodies of differentiated achondrites (angrites, eucrites), we analyzed two shergottites (Zagami, DaG 476), three angrites (NWA 4801, NWA 4590, D'Orbigny) and four eucrites (Stannern, Bereba, Millbillillie, Dhofar 007). Among these samples, three (NWA 4801, DaG 476, Bereba) exhibit very heavy Mo isotope compositions, which are well above the threshold of $\delta^{98/95}\mathrm{Mo} = +0.14‰$ for signatures of core formation (see above). Both NWA 4801 and DaG 476 are desert finds and, hence, their Mo isotope compositions may be affected by terrestrial weathering. In oxidizing environments such as the Earth's surface, Mo is easily mobilized as molybdate oxyanions, and weathering has indeed been shown to fractionate Mo isotopes (Goldberg et al., 2009). A study of the Mo isotope composition of major rivers indicates a net enrichment in heavy Mo isotopes during weathering of crustal rocks (Archer and Vance, 2008). It is likely that similar processes occurred during terrestrial weathering of meteorites. However, the multitude of reactions involved (adsorption and desorption reactions on multiple phases; flux of Mo ions in and out of the meteorite) does not allow predictions about the magnitude and direction of Mo isotope fractionation in these rocks, without analyzing specifically the alteration phases. In any case, the heavy Mo isotope composition of Béreba, and also that of Millbillillie – both observed meteorite falls – are unlikely caused by terrestrial weathering, indicating that their $\delta^{98/95}\mathrm{Mo}$ values reflect processes on the eucrite parent body. Note that the $\delta^{98/95}\mathrm{Mo}$ values of these eucrites (and that of Dhofar 007) are too high to be the sole result of core formation. Thus, partial melting and/or impact and thermal metamorphism may be responsible for the elevated and variable $\delta^{98/95}\mathrm{Mo}$ of the eucrites. Note that eucrites experienced a complex probably fluid-driven and metal-forming thermal metamorphism (Warren et al., 2013). This highlights that using Mo isotopes as a tracer of core formation requires a detailed understanding of any post-core formation Mo isotope fractionation.

The $\delta^{98/95}$Mo of -0.10 ± 0.07 for Zagami is slightly heavier than, albeit not resolved from chondrites and would translate into a metal–silicate equilibration temperature of 2490 ± 770 °C, which given its relatively large uncertainty is in acceptable agreement with a core formation temperature of 1830 ± 200 °C that has been estimated based on the depletions of siderophile elements in the martian mantle (Righter and Chabot, 2011). However, given the evidence for post-core formation Mo isotope fractionation in eucrites, the $\delta^{98/95}$Mo value of Zagami may not solely result from core formation.

All three investigated angrites are finds, such that terrestrial weathering may have affected their Mo isotope compositions. However, D'Orbigny appears to be very fresh (Grossman and Zipfel, 2001) and was not subjected to the prolonged desert weathering that has affected NWA 4590 and NWA 4801. The $\Delta^{98/95}Mo_{bulk\text{-}silicate}$ of D'Orbigny is -0.11 ± 0.05‰, which translates to a metal–silicate equilibration temperature of 1790 ± 230 °C. This temperature agrees with estimates inferred using siderophile element depletions (Shirai et al., 2009) and is well above the peridotite liquidus for even the largest asteroids (Agee, 1997) and thus indicates core formation by efficient metal–silicate separation and metal segregation during large-scale melting. This in turn is consistent with the early timing of core formation as deduced from Hf–W data, indicating that at the time of parent body accretion ^{26}Al was sufficiently abundant to cause melting (Kleine et al., 2012), and with the presence of a core-dynamo for at least ~10 Myr (Weiss et al., 2008).

4.4.3. Earth

The four terrestrial samples investigated in this study have $\delta^{98/95}$Mo values ranging from chondritic (Dolerite DNC-1, $\delta^{98/95}$Mo $= -0.18 \pm 0.06$‰) to values ~0.1‰ heavier than the bulk $\delta^{98/95}$Mo of inner solar system bodies, averaging at -0.1 ± 0.1‰ (2 s.d.). Siebert et al. (2003) reported Mo isotope data for several subduction-related volcanic rocks from Kamchatka and for Himalayan granites. Renormalizing their data to the SRM3134 standard using the conversion of Greber et al. (2012) gives a mean $\delta^{98/95}$Mo $= -0.17 \pm 0.22$ (2 s.d.), within the range of Mo isotope compositions for terrestrial samples obtained in the present study. More recently, Liang et al. (2013) reported Mo isotope data for a suite of mafic and ultramafic rocks and on the basis of these data argued that the $\delta^{98/95}$Mo of the bulk silicate Earth is $+0.38 \pm 0.15$‰ (relative to SRM3134). However, this value is above the maximum $\delta^{98/95}$Mo $= +0.14$‰ permissible for core formation and, therefore, cannot easily represent the Mo isotope composition of the bulk silicate Earth. Collectively, the available Mo isotope data for terrestrial igneous rocks indicate that there are mass-dependent Mo isotope variations of more than ~0.1‰ among terrestrial igneous rocks, making it difficult to precisely estimate the $\delta^{98/95}$Mo characteristic for the bulk silicate Earth. However, based on the bulk Earth $\delta^{98/95}$Mo $= -0.16 \pm 0.02$‰ inferred in the present study, the experimentally determined Mo isotope fractionation factor between metal and silicate from Hin et al. (2013), and independent estimates for the mean temperature of core formation in the Earth, a reasonable range of expected $\delta^{98/95}$Mo values for the bulk silicate Earth can be estimated. For instance, for metal–silicate equilibration temperatures >2500 °C (Rubie et al., 2007; Wood et al., 2006; Siebert et al., 2013) $\delta^{98/95}$Mo values of less than -0.1‰ would be predicted for the bulk silicate Earth. Obviously, the metal–silicate equilibration temperatures may have been lower, because the formation of Earth's core may have involved incomplete equilibration of newly accreted bodies with the terrestrial mantle (e.g., Kleine et al., 2009; Rudge et al., 2010; Stevenson, 2008). In this case, slightly higher $\delta^{98/95}$Mo values would be expected. However, we note that $\delta^{98/95}$Mo > 0 for the bulk silicate Earth is unlikely, as this would imply unrealistically low core formation temperatures of less than ~1400 °C. Clearly, precisely defining the $\delta^{98/95}$Mo value characteristic for the bulk silicate Earth can provide essential constraints on the conditions of core formation in the Earth, but will require further work and most of all a detailed understanding of the processes that fractionated Mo isotopes in terrestrial igneous rocks.

5. Conclusions

Our measurements indicate that mass-dependent Mo isotope fractionation occurs at high temperatures by processes within the solar nebula and during planetary differentiation. Most chondrites and iron meteorites exhibit indistinguishable Mo isotope compositions and as such define the $\delta^{98/95}$Mo of bulk planetary bodies in the inner solar system. Chondrites that formed under highly oxidized conditions (such as the CM, CK chondrites) deviate from the bulk $\delta^{98/95}$Mo of the inner solar system and exhibit heavier Mo isotope compositions. This probably reflects either evaporative losses of volatile and isotopically light Mo oxides, or a heterogeneous distribution of an isotopically light metal and/or an isotopically heavy matrix component. Molybdenum isotope data for chondrite components are needed for establishing the origin of isotope fractionation among bulk carbonaceous chondrites, however. The Mo isotope composition of the IAB iron meteorites also deviates from the bulk $\delta^{98/95}$Mo of the inner solar system, and this most likely is due to impact-induced losses of isotopically light Mo.

Most of the samples from the silicate portions of differentiated bodies are isotopically heavier than the bulk planets, which at least in part is due to Mo isotope fractionation during metal–silicate equilibration. However, some samples exhibit Mo isotope compositions that are too heavy to solely result from core formation, indicating that other processes such as partial melting or thermal and impact metamorphism also led to Mo isotope fractionation. For the Moon such post-core formation Mo isotope fractionation seems to have been minor to absent and so the lunar Mo isotope data can be used to estimate a temperature of metal–silicate equilibration during segregation of the lunar core. The resulting temperature of 1800 ± 200 °C is in excellent agreement with other, independent estimates of core formation temperatures for the Moon. The temperature estimates for the angrite parent body (1790 ± 230 °C) and Mars (2500 ± 770 °C) are more uncertain, because the magnitude and direction of post-core formation Mo isotope fractionation on these bodies are not known. Our study together with the companion study of Hin et al. (2013) demonstrates the great potential of mass-dependent Mo isotope fractionation to constrain the conditions of core formation in asteroids and terrestrial planets, but also highlights the difficulty in determining the $\delta^{98/95}$Mo characteristic for the bulk silicate portion of a differentiated body. Thus, the application of Mo isotopes to constrain core formation most of all requires an improved understanding of potential Mo isotope fractionation during post-core formation processes.

Acknowledgements

This work was supported by the SNF (No. 2-77213-08). We thank M. Fischer-Gödde, T. Kruijer and D. Cook for assistance with setting up Mo measurements in Münster, Frank Richter for discussions about isotope fractionation in the solar nebula, an anonymous reviewer and Dimitri Papanasstassiou for helpful comments and the editor Bernard Marty for the handling of the manuscript.

Appendix A. Supplementary material

Supplementary material related to this article can be found online at http://dx.doi.org/10.1016/j.epsl.2014.01.037.

References

Agee, C., 1997. Melting temperatures of the Allende meteorite: Implications for a Hadean magma ocean. Phys. Earth Planet. Inter. 100, 41–47.

Anbar, A., 2004. Molybdenum stable isotopes: Observations, interpretations and directions. In: Johnson, C.M., Beard, B.L., Albarede, F. (Eds.), Rev. Mineral. Geochem., vol. 55. Mineralogical Society of America, pp. 429–454.

Archer, C., Vance, D., 2008. The isotopic signature of the global riverine molybdenum flux and anoxia in the ancient oceans. Nat. Geosci. 1, 597–600.

Arlandini, C., Käppeler, F., Wisshak, K., 1999. Neutron capture in low-mass asymptotic giant branch stars: cross sections and abundance signatures. Astrophys. J. 525, 886–900.

Armytage, R.M.G., Georg, R.B., Savage, P.S., Williams, H.M., Halliday, A.N., 2011. Silicon isotopes in meteorites and planetary core formation. Geochim. Cosmochim. Acta 75, 3662–3676.

Armytage, R.M.G., Georg, R.B., Williams, H.M., Halliday, A.N., 2012. Silicon isotopes in lunar rocks: Implications for the Moon's formation and the early history of the Earth. Geochim. Cosmochim. Acta 77, 504–514.

Benedix, G., McCoy, T., Keil, K., Love, S.G., 2000. A petrologic study of the IAB iron meteorites: Constraints on the formation of the IAB-winonaite parent body. Meteorit. Planet. Sci. 35, 1127–1141.

Burkhardt, C., Kleine, T., Dauphas, N., Wieler, R., 2012. Origin of isotopic heterogeneity in the solar nebula by thermal processing and mixing of nebular dust. Earth Planet. Sci. Lett. 357–358, 298–307.

Burkhardt, C., Kleine, T., Oberli, F., Pack, A., Bourdon, B., Wieler, R., 2011. Molybdenum isotope anomalies in meteorites: Constraints on solar nebula evolution and origin of the Earth. Earth Planet. Sci. Lett. 312, 390–400.

Canup, R.M., 2004. Dynamics of lunar formation. Annu. Rev. Astron. Astrophys. 42, 441–475.

Canup, R.M., 2012. Forming a Moon with an Earth-like composition via a giant impact. Science 338, 1052–1055.

Chapman, S., Cowling, T.G., 1970. The Mathematical Theory of Non-Uniform Gases. Cambridge University Press.

Charlier, B.L.A., Nowell, G.M., Parkinson, I.J., Kelley, S.P., Pearson, D.G., Burton, K.W., 2012. High temperature strontium stable isotope behaviour in the early solar system and planetary bodies. Earth Planet. Sci. Lett. 329, 31–40.

Chen, H., Nguyen, B.M., Moynier, F., 2013. Zinc isotopic composition of iron meteorites: Absence of isotopic anomalies and origin of the volatile element depletion. Meteorit. Planet. Sci. 48, 2441–2450.

Choi, B.G., Ouyang, X.W., Wasson, J.T., 1995. Classification and origin of IAB and IIICD iron meteorites. Geochim. Cosmochim. Acta 59, 593–612.

Cuk, M., Stewart, S.T., 2012. Making the Moon from a fast-spinning Earth: A giant impact followed by resonant despinning. Science 338, 1047–1052.

Dauphas, N., Davis, A.M., Marty, B., Reisberg, L., 2004. The cosmic molybdenum–ruthenium isotope correlation. Earth Planet. Sci. Lett. 226, 465–475.

Dauphas, N., Marty, B., Reisberg, L., 2002. Molybdenum evidence for inherited planetary scale isotope heterogeneity of the protosolar nebula. Astrophys. J. 565, 640–644.

Fegley, B., Palme, H., 1985. Evidence for oxidizing conditions in the solar nebula from Mo and W depletions in refractory inclusions in carbonaceous chondrites. Earth Planet. Sci. Lett. 72, 311–326.

Fitoussi, C., Bourdon, B., 2012. Silicon isotope evidence against an enstatite chondrite Earth. Science 335, 1477–1480.

Fitoussi, C., Bourdon, B., Kleine, T., Oberli, F., Reynolds, B.C., 2009. Si isotope systematics of meteorites and terrestrial peridotites: implications for Mg/Si fractionation in the solar nebula and for Si in the Earth's core. Earth Planet. Sci. Lett. 287, 77–85.

Gao, X., Thiemens, M.H., 1993. Variations of the isotopic composition of sulfur in enstatite and ordinary chondrites. Geochim. Cosmochim. Acta 57, 3171–3176.

Georg, R.B., Halliday, A.N., Schauble, E.A., Reynolds, B.C., 2007. Silicon in the Earth's core. Nature 447, 1102–1106.

Goldberg, T., Archer, C., Vance, D., Poulton, S.W., 2009. Mo isotope fractionation during adsorption to Fe (oxyhydr)oxides. Geochim. Cosmochim. Acta 73, 6502–6516.

Greber, N.D., Siebert, C., Nägler, T.F., Pettke, T., 2012. δ98/95Mo values and molybdenum concentration data for NIST SRM 610, 612 and 3134: Towards a common protocol for reporting Mo data. Geostand. Geoanal. Res. 36, 291–300.

Grossman, J.N., Zipfel, J., 2001. The Meteoritical Bulletin, No. 85, 2001 September. Meteorit. Planet. Sci. 36, A293–A322.

Hin, R.C., Burkhardt, C., Schmidt, M.W., Bourdon, B., Kleine, T., 2013. Experimental evidence for Mo isotope fractionation between metal and silicate liquids. Earth Planet. Sci. Lett. 379, 38–48.

Hin, R.C., Fitoussi, C., Schmidt, M.W., Bourdon, B., 2014. Experimental determination of the Si isotope fractionation factor between liquid metal and liquid silicate. Earth Planet. Sci. Lett. 387, 55–66.

Holzheid, A., Palme, H., 2007. The formation of eucrites: Constraints from metal–silicate partition coefficients. Meteorit. Planet. Sci. 42, 1817–1829.

Humayun, M., Clayton, R.N., 1995. Precise determination of the isotopic composition of potassium – application to terrestrial rocks and lunar soils. Geochim. Cosmochim. Acta 59, 2115–2130.

Kleine, T., Hans, U., Irving, A., Bourdon, B., 2012. Chronology of the angrite parent body and implications for core formation in protoplanets. Geochim. Cosmochim. Acta 84, 186–203.

Kleine, T., Mezger, K., Münker, C., Palme, H., Bischoff, A., 2004. ^{182}Hf–^{182}W isotope systematics of chondrites, eucrites, and Martian meteorites: Chronology of core formation and mantle differentiation in Vesta and Mars. Geochim. Cosmochim. Acta 68, 2935–2946.

Kleine, T., Touboul, M., Bourdon, B., Nimmo, F., Mezger, K., Palme, H., Yin, Q.Z., Jacobsen, S.B., Halliday, A.N., 2009. Hf–W chronology of the accretion and early evolution of asteroids and terrestrial planets. Geochim. Cosmochim. Acta 73, 5150–5188.

Kracher, A., 1985. The evolution of partially differentiated planetesimals: evidence from iron meteorite groups IAB and IIICD. In: Proc. 15th Lunar Planet. Sci. Conf, pp. 689–698.

Krot, A.N., Keil, K., Scott, E.R.D., Goodrich, C.A., Weisberg, M.K., 2007. Classification of meteorites. In: Holland, H.D., Turekian, K.K. (Eds.), Treatise on Geochemistry, vol. 1. Pergamon, pp. 1–52.

Liang, Y., Siebert, C., Fritton, J.G., Burton, K.W., Hallyday, A.N., 2013. Molybdenum isotope fractionation in the mantle. In: Goldschmidt Conference 2013. #5365.

Luais, B., 2007. Isotopic fractionation of germanium in iron meteorites: Significance for nebular condensation, core formation and impact processes. Earth Planet. Sci. Lett. 262, 21–36.

Luck, J., Othman, D.B., Albaréde, F., 2005. Zn and Cu isotopic variations in chondrites and iron meteorites: Early solar nebula reservoirs and parent-body processes. Geochim. Cosmochim. Acta 69, 5351–5363.

Magna, T., Wiechert, U., Halliday, A., 2006. New constraints on the lithium isotope compositions of the Moon and terrestrial planets. Earth Planet. Sci. Lett. 243, 336–353.

Moynier, F., Agranier, A., Hezel, D., Bouvier, A., 2010. Sr stable isotope composition of Earth, the Moon, Mars, Vesta and meteorites. Earth Planet. Sci. Lett. 300, 359–366.

Moynier, F., Albarède, F., Herzog, G.F., 2006. Isotopic composition of zinc, copper, and iron in lunar samples. Geochim. Cosmochim. Acta 70, 6103–6117.

Moynier, F., Yin, Q.Z., Schauble, E., 2011. Isotopic evidence of Cr partitioning into Earth's core. Science 331, 1417–1420.

Neal, C.R., 2001. Interior of the Moon: the presence of garnet in the primitive deep lunar parent body. J. Geophys. Res. 106, 27865–27885.

Newsom, H.E., 1985. Molybdenum in eucrites – evidence for a metal core in the eucrite parent body. J. Geophys. Res. 90, 613–617.

Newsom, H.E., 1986. Constraints on the origin of the Moon from the abundance of molybdenum and other siderophile elements. In: Hartmann, W.K., Phillips, R.J., Taylor, G.J. (Eds.), Origin of the Moon, pp. 203–229.

Newsom, H.E., Palme, H., 1984. The depletion of siderophile elements in the Earth's mantle: new evidence from molybdenum and tungsten. Earth Planet. Sci. Lett. 69, 354–364.

Niederer, F.R., Papanastassiou, D.A., Wasserburg, G.J., 1985. Absolute isotopic abundances of Ti in meteorites. Geochim. Cosmochim. Acta 49, 835–851.

O'Neill, H.S.C., 1991. The origin of the moon and the early history of the Earth – a chemical model. Part 2: The Earth. Geochim. Cosmochim. Acta 55, 1159–1172.

Palme, H., O'Neill, H.S.C., 2003. Cosmochemical estimates of mantle composition. In: Holland, H., Turekian, K.K. (Eds.), Treatise on Geochemistry, vol. 2. Elsevier, Amsterdam, pp. 1–38.

Patchett, P.J., 1980. Sr isotopic fractionation in Allende chondrules – a reflection of solar nebular processes. Earth Planet. Sci. Lett. 50, 181–188.

Patchett, P.J., Tatsumoto, M., 1980. A routine high-precision method for Lu–Hf isotope geochemistry and chronology. Contrib. Mineral. Petrol. 75, 263–267.

Reufer, A., Meier, M.M.M., Benz, W., Wieler, R., 2012. A hit-and-run giant impact scenario. Icarus 221, 296–299.

Righter, K., 2002. Does the Moon have a metallic core? Constraints from giant impact modeling and siderophile elements. Icarus 158, 1–13.

Righter, K., Chabot, N., 2011. Moderately and slightly siderophile element constraints on the depth and extent of melting in early Mars. Meteorit. Planet. Sci. 46, 157–176.

Righter, K., Hervig, R.L., Kring, D.A., 1998. Accretion and core formation on Mars: Molybdenum contents of melt inclusion glasses in three SNC meteorites. Geochim. Cosmochim. Acta 62, 2167–2177.

Rubie, D.C., Nimmo, F., Melosh, H.J., 2007. Formation of Earth's core. In: Treatise on Geochemistry, vol. 9. Elsevier, pp. 51–90.

Rudge, J., Kleine, T., Bourdon, B., 2010. Broad bounds on Earth's accretion and core formation constrained by geochemical models. Nat. Geosci. 3, 439–443.

Rudge, J.F., Reynolds, B.C., Bourdon, B., 2009. The double spike toolbox. Chem. Geol. 265, 420–431.

Savage, P.S., Moynier, F., 2013. Silicon isotopic variation in enstatite meteorites: Clues to their origin and Earth-forming material. Earth Planet. Sci. Lett. 361, 487–496.

Shahar, A., Hillgren, V.J., Young, E.D., Fei, Y.W., Macris, C.A., Deng, L.W., 2011. High-temperature Si isotope fractionation between iron metal and silicate. Geochim. Cosmochim. Acta 75, 7688–7697.
Shirai, N., Humayun, M., Righter, K., 2009. Analysis of moderately siderophile elements in angrites: implications for core formation of the angrite parent body. In: 40th Lunar and Planetary Science Conference. #2122.
Siebert, J., Badro, J., Antonangeli, D., Ryerson, F., 2013. Terrestrial accretion under oxidizing conditions. Science 339, 1194–1197.
Siebert, C., Nagler, T., Kramers, J., 2001. Determination of molybdenum isotope fractionation by double-spike multicollector inductively coupled plasma mass spectrometry. Geochem. Geophys. Geosyst. 2. Art. No. 2000GC000124.
Siebert, C., Nagler, T., von Blankenburg, F., Kramers, J., 2003. Molybdenum isotope records as a potential new proxy for paleoceanography. Earth Planet. Sci. Lett. 211, 159–171.
Simon, J.I., DePaolo, D.J., 2010. Stable calcium isotopic composition of meteorites and rocky planets. Earth Planet. Sci. Lett. 289, 457–466.
Stevenson, D., 2008. A planetary perspective on the deep Earth. Nature 451, 261–265.
Touboul, M., Kleine, T., Bourdon, B., Palme, H., Wieler, R., 2007. Late formation and prolonged differentiation of the Moon inferred from W isotopes in lunar metals. Nature 450, 1206–1209.
Wade, J., Wood, B.J., Tuff, J., 2012. Metal–silicate partitioning of Mo and W at high pressures and temperatures: Evidence for late accretion of sulphur to the Earth. Geochim. Cosmochim. Acta 85, 58–74.
Walter, M.J., Thibault, Y., 1995. Partitioning of tungsten and molybdenum between metallic liquid and silicate melt. Science 270, 1186–1189.
Warren, P.H., Isa, J., Gessler, N., 2013. Petrology of secondary mineral development, probably fluid-driven, within the uniquely evolved eucrite Northwest Africa 5738. In: 44th Lunar and Planetary Science Conference. #2875.
Wasson, J.T., 1985. Meteorites: Their Record of Early-Solar System History. W.H. Freeman and Company.
Weber, R., Lin, P., Garnero, E., Williams, Q., Lognonné, P., 2011. Seismic detection of the lunar core. Science 331, 309–312.
Weiss, B., Berdahl, J., Elkins-Tanton, L., Stanley, S., Lima, E., Carporzen, L., 2008. Magnetism on the angrite parent body and the early differentiation of planetesimals. Science 322, 713–716.
Wombacher, F., Rehkämper, M., Mezger, K., Bischoff, A., Münker, C., 2008. Cadmium stable isotope cosmochemistry. Geochim. Cosmochim. Acta 72, 646–667.
Wood, B.J., Walter, M.J., Wade, J., 2006. Accretion of the Earth and segregation of its core. Nature 441, 825–833.